

patients with atherosclerosis. This has encouraged our group and others to verify experimentally whether EPC-seeded vascular grafts provide high patency similar to that of EC-seeded grafts. Two grafts have been investigated: one is a canine EPC-seeded compliant graft⁸ and the other is a sheep EPC-seeded decellularized vessel.⁹

Although it would be interesting to compare the proliferative and antithrombogenic potentials of EPCs with those of ECs, little study has been conducted thus far. Therefore, the present study aims to resolve this issue, which is necessary to provide a logical or rational basis for the construction of an EPC-based engineered graft. First, the proliferation characteristics of EPCs were determined, followed by the quantitative determination of the expression of antithrombogenic substances such as endothelial nitric oxide synthase (eNOS),¹⁰ prostaglandin I₂ (PGI₂),¹¹ and tissue-type plasminogen activator (tPA).¹² The former two substances exhibit potent antiplatelet activity and the latter substance has fibrinolytic activity. Last, to realize an EPC-seeded engineered graft, an EPC-seeded compliant small-diameter graft was subjected to *ex vivo* hydrodynamic circulation simulating arterial blood flow, which is expected to ensure cell-matrix and cell-cell interactions.^{13,14}

MATERIALS AND METHODS

Isolation of mononuclear cells from human peripheral blood

Approximately 100 mL of human peripheral blood from healthy adult subjects was collected from the

cephalic vein into plastic syringes containing 1000 USP of sodium heparin. The median age of the subjects ($n = 11$) was 29 years (range, 22–33 years). The blood was diluted 1:1 with isolation buffer (Dulbecco's phosphate-buffered saline [PBS] supplemented with 2 mM EDTA) and the diluted solution was gently layered over a Ficoll gradient (Histopaque-1077; Sigma, St. Louis, MO) and subsequently centrifuged at $400 \times g$ for 30 min at 25°C. Subsequently, peripheral blood mononuclear cells (PBMCs) were obtained and washed by diluting the isolation buffer and centrifuging at $250 \times g$ for 10 min at 4°C.

Cell culture

PBMCs were suspended in EC basal medium 2 (Clonetics, San Diego, CA) supplemented with 20% fetal bovine serum (Life Technologies, Rockville, MD) and with 0.94% EGM-2 MV (Clonetics), which contained human vascular endothelial growth factor, human fibroblast growth factor, human epidermal growth factor, insulin-like growth factor I, ascorbic acid, and hydrocortisone acetate. To exclude monocytes and macrophages, the cells were seeded in a polystyrene dish (cell culture dish, 100 × 20 mm; Corning, Corning, NY) with the same medium and were incubated for 1 h at 37°C. Unattached cells were collected and seeded in the same medium in a polystyrene dish coated with fibronectin (0.1 mg/mL; Sigma). Cultures were incubated at 37°C in a humidified environment with 5% CO₂. After 3 days of culture, all culture medium was exchanged and thereafter the medium was exchanged three times a week. At 3 to 4

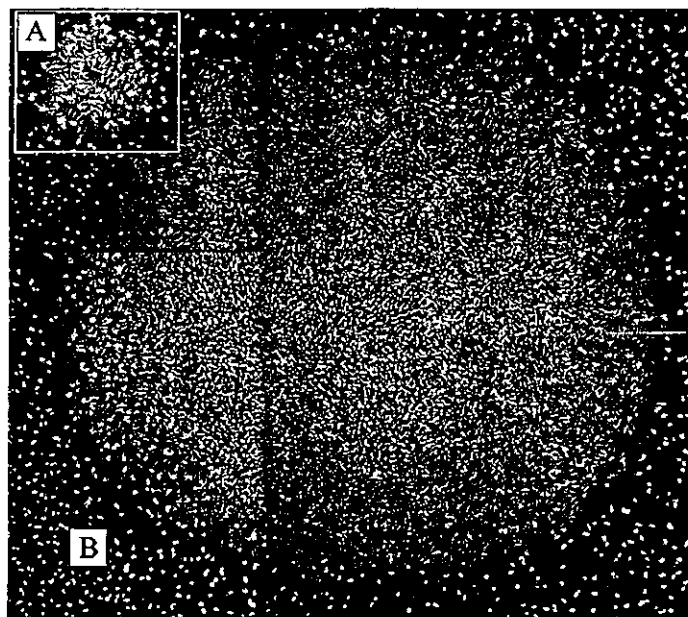


FIG. 1. Phase-contrast light micrographs of a primary culture of human peripheral blood mononuclear cell (PBMC)-derived EC-like cells. Small-sized cobblestone-like cell colonies appeared within 2 weeks of plating and rapidly grew with culture time [after culture for (A) 12 days and (B) 18 days]. Original magnification, $\times 40$; bar, 0.5 mm.

weeks of culture, the outgrown EC-like cell colonies were subcultured with 0.1% trypsin (Life Technologies) in a 100-mm cell culture dish and these cells were expanded until confluence. Expanded cells were collected with 0.1% trypsin. Among the second-passage cells, 4.0×10^4 cells were used for determination of cell growth, and the rest of the cells were continued in culture for cell characterization.

Measurement of growth kinetics of EC-like cells

The collected second-passage cells mentioned above were seeded into 4 wells of a 24-well culture plate (Corning) at a seeding density of 5×10^3 cells/cm². The cell numbers were quantified on the basis of phase-contrast micrographs (Eclipse TE 300; Nikon, Tokyo, Japan) taken randomly at 10 areas of each of the 4 wells. Growth curves and population doubling times (PDT) were calculated from the average cell number of four wells at the exponential stage (24 to 120 h after seeding). To exclude the effect of initial cell density on cell growth, the growth of some cells was requantified at a lower seeding cell density (5×10^2 cells/cm²).

Characterization of EC-like cells

To identify EC-like cells in cultures of PBMCs as endothelial lineage cells, the cellular expression of von Willebrand factor (vWF) and Flk-1 (vascular endothelial growth factor receptor 2) was examined. EC-like cells from cultures and human umbilical vein endothelial cells (HUVECs) as positive control were grown on chamber slides (Lab-Tek chamber slides; Nalge Nunc, Naperville, IL) and fixed with fix solution (1% glutaraldehyde-1.44% paraformaldehyde in buffer) for 30 min at 37°C. As the primary antibodies, rabbit polyclonal antibody against human vWF (Nichirei, Tokyo, Japan) and mouse IgG against human Flk-1 (Santa Cruz Biotechnology, Santa Cruz, CA) were applied to the cells. After washing with PBS, biotinylated goat anti-rabbit IgG antibody (Nichirei) for vWF detection or biotinylated rabbit polyclonal anti-mouse antibody (Nichirei) for Flk-1 detection was applied. After washing with PBS, streptavidin combined with immunoperoxidase (Nichirei) was applied, and finally 3,3'-diaminobenzidine-tetrahydrochloride (Merck, Darmstadt, Germany) was used to visualize the immunoreaction products. The percentages of positive cells were obtained by calculating the number of positive

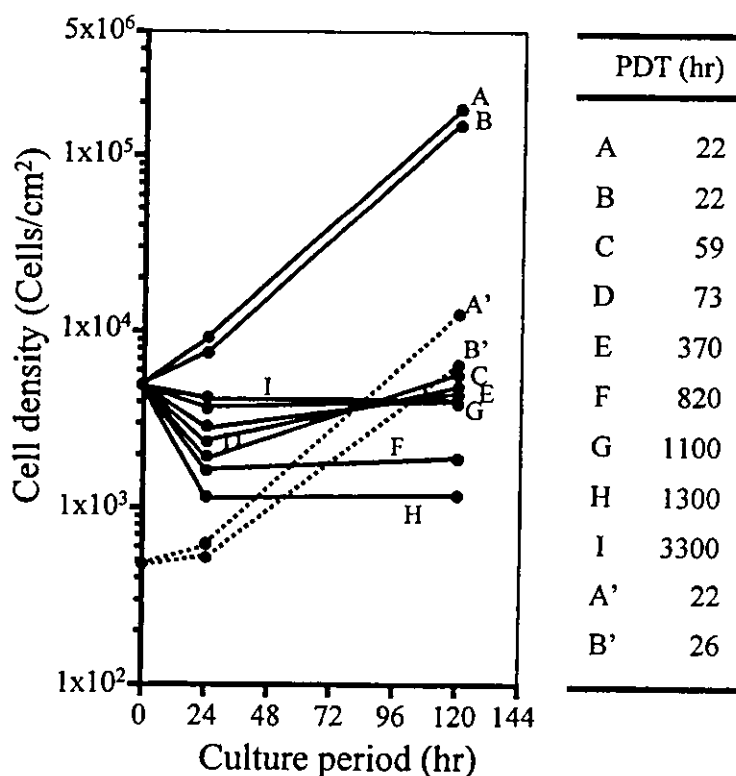


FIG. 2. Growth kinetics of human PBMC-derived EC-like cells from nine samples. *Left:* Growth curves of EC-like cells from nine samples. The cells were initially seeded at 5×10^3 cells/cm², and cells were counted 24 and 120 h after seeding. Only two cell types (A and B) gave highly proliferative potentials. A' and B' (dotted lines) indicate growth curves in which cell types A and B were seeded at a low initial cell density (5×10^2 cells/cm²), respectively. *Right:* Population doubling times (PDTs) of EC-like cells calculated from the cell numbers 24 and 120 h after seeding.

cells (total number of counted cells, 1000) under a light microscope.

To evaluate cellular uptake of acetylated low-density lipoprotein (LDL), EC-like cells cultured on chamber slides were incubated in medium containing 20 $\mu\text{L}/\text{mL}$ 1,1'-dioctadecyl-3,3,3',3'-tetramethylindocarbocyanine perchlorate (DiI)-3 labeled acetylated LDL (Biomedical Technologies, Stoughton, MA) for 4 h at 37°C. Cells were examined under a confocal laser-scanning microscope (CLSM) (Radiance 2000; Bio-Rad, Hercules, CA) after washing with PBS.

Diamino-fluorescein-2-diacetate (DAF-2DA; Daiichi Pure Chemicals, Tokyo, Japan), which is a membrane-permeable intracellular nitric oxide (NO)-specific fluorescent indicator, was used to detect NO expression.¹⁵ EC-like cells were washed twice with Hanks' balanced salt solution (Life Technologies) and then immersed in serum-free M199 (Life Technologies) medium containing 10 μM DAF-2DA. After 60 min of incubation at 37°C, cells were washed twice with PBS and fixed. When DAF-2DA reacted with NO, green fluorescent triazole was yielded. Cells subjected to the above-mentioned procedure were examined under a CLSM.

Immunoassay for human eNOS, PGI₂, and tPA

The amount of cellular eNOS was quantified immunochemically with an enzyme-linked immunosorbent assay kit (AN'ALYZA-human eNOS; Genzyme, Minneapolis, MN). Third-passage, confluent EC-like cells and HUVECs were suspended in PBS, and lysed with cell lysis buffer from the kit. The assays were performed with 1×10^6 cells. 6-Keto-prostaglandin-F₁- α (6-keto-PGF₁- α), which is a degenerative product of PGI₂, and tPA, both of which are secreted by cultured third-passage EC-like cells and HUVECs at confluence into the supernatant for 24 h, were quantified immunochemically with the corresponding enzyme-linked immunosorbent assay kit (tPA, Imulyse tPA [Biopool, Umea, Sweden] and PGI₂, Correlate-EIA 6-keto-prostaglandin-F₁- α enzyme immunoassay kit [Assay Designs, Ann Arbor, MI]). Comparisons between the two groups of data for eNOS, 6-keto-PGF₁- α , and tPA were performed with the nonpaired Student *t* test; significant differences were defined as $p < 0.05$.

Fabrication of artificial vascular graft

The fabrication of microporous grafts coated with photoreactive gelatin was performed according to procedures previously reported.¹⁶ Briefly, a tubular film (internal diameter, 1.5 mm; wall thickness, 100 μm) of segmented polyurethane (SPU) (Cardiomat 610; Kontron Instruments, Boston, MA) was prepared by dip coating a glass rod into a tetrahydrofuran-dioxan solution of SPU. The tube was multiply pored (pore size, 100 μm ; longitudi-

nal pore-to-pore distance, 200 μm ; circumferential pore-to-pore interval, 15°) by pulsed UV light irradiation, using a KrF excimer laser microprocessing apparatus (C4500, C4540; Hamamatsu Photonics, Hamamatsu, Japan). Both outer and luminal surfaces of the microporous SPU tube were coated with an aqueous solution of photoreactive gelatin (20 mg/mL), which was partially derivatized with photoinduced radicals producing the benzophenone group (the detailed preparation procedure is described in a previous article¹⁶), and were subsequently irradiated with UV light for 10 min. EC-like cells of confluent cultures were harvested and diluted with 0.3 mL of the culture medium (total cell number, 5×10^5 cells). The cell suspension was added to the photogelled microporous SPU graft (length, 20 mm), and subsequently immersed in the culture medium for 1 h at 37°C. Another cell suspension was then added in the same manner and the graft was rotated 120° around its

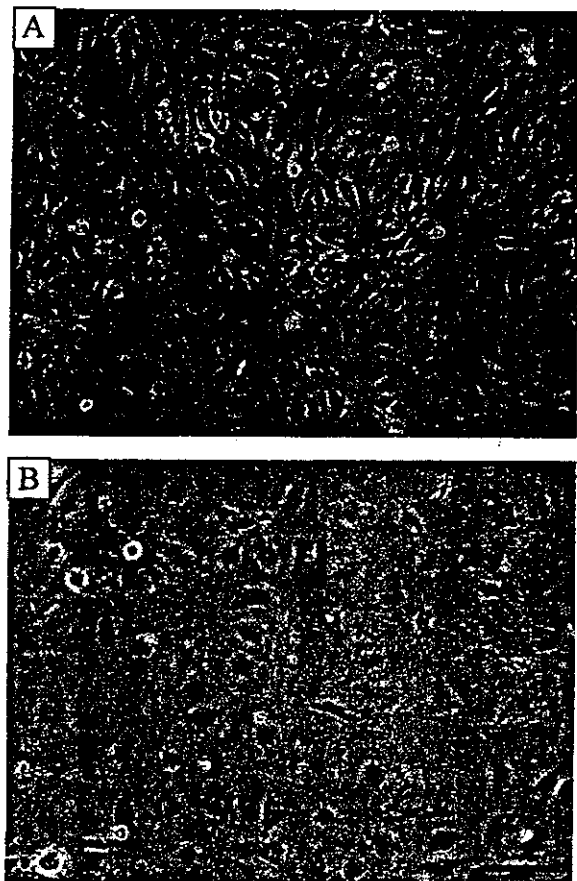


FIG. 3. (A) Phase-contrast photomicrograph of EC-like cells with a doubling time of 22 h (second passage of primary culture), showing a polygonal cell monolayer constructed of small cells. (B) Phase-contrast photomicrograph of human PBMC-derived EC-like cells with a population doubling time of 59 h (second passage of primary culture), showing large and bizarre morphology (original magnification, $\times 100$; bar, 100 μm).

longitudinal axis. After repeating this procedure three times (total seeded cells, 1.5×10^5 cells/graft; cell density, 8.0×10^4 cells/cm²), the graft was incubated for 4 days to ensure complete monolayer formation.

Shear stress experiment

Hydrodynamic shear stress loading on adherent seeded cells in grafts (length, 2 cm) was carried out as follows. The cell-seeded graft was connected to a circulatory loop system. The circulatory loop consists of a roller pump (RP-NE3; Furue Science, Tokyo, Japan) upstream of the graft, and an outflow reservoir downstream of the graft. The graft was tied to the circulatory loop, and the circulatory loop was filled with culture medium. Medium flowed from the roller pump through the graft and into the outflow reservoir. Medium in the outflow reservoir was pumped up with the roller pump and recirculated. The entire apparatus except for the roller pump was installed in an incubator at 37°C in a humidified environment with 5% CO₂. The pump setting was 70 strokes/min, which yielded a flow rate of 60 mL/min. At this flow

rate, the calculated shear stress at the graft was 30 dyn/cm². The flow system was run for 12 h. The graft was then immersed in fix solution.

RESULTS

Proliferation of EC-like cells derived from peripheral blood

After PBMCs were isolated according to the method previously mentioned, PBMCs were cultured in 20% FBS-containing EC basal medium 2 supplemented with 0.94% EGM-2 MV (multicomponents of growth factors) on fibronectin-coated dishes. Nine of 11 samples examined produced outgrowing, EC-like colonies (82%), and the rest of the adherent cells such as monocytes and rod-like cells died over time, within 2 to 4 weeks. The number of colonies ranged from one to four per PBMC sample from 100 mL of blood. Two patterns of proliferation were observed: in one, a small colony appeared approximately 10 to 21 days after plating, and the size of that colony rapidly expanded with time. This is exemplified

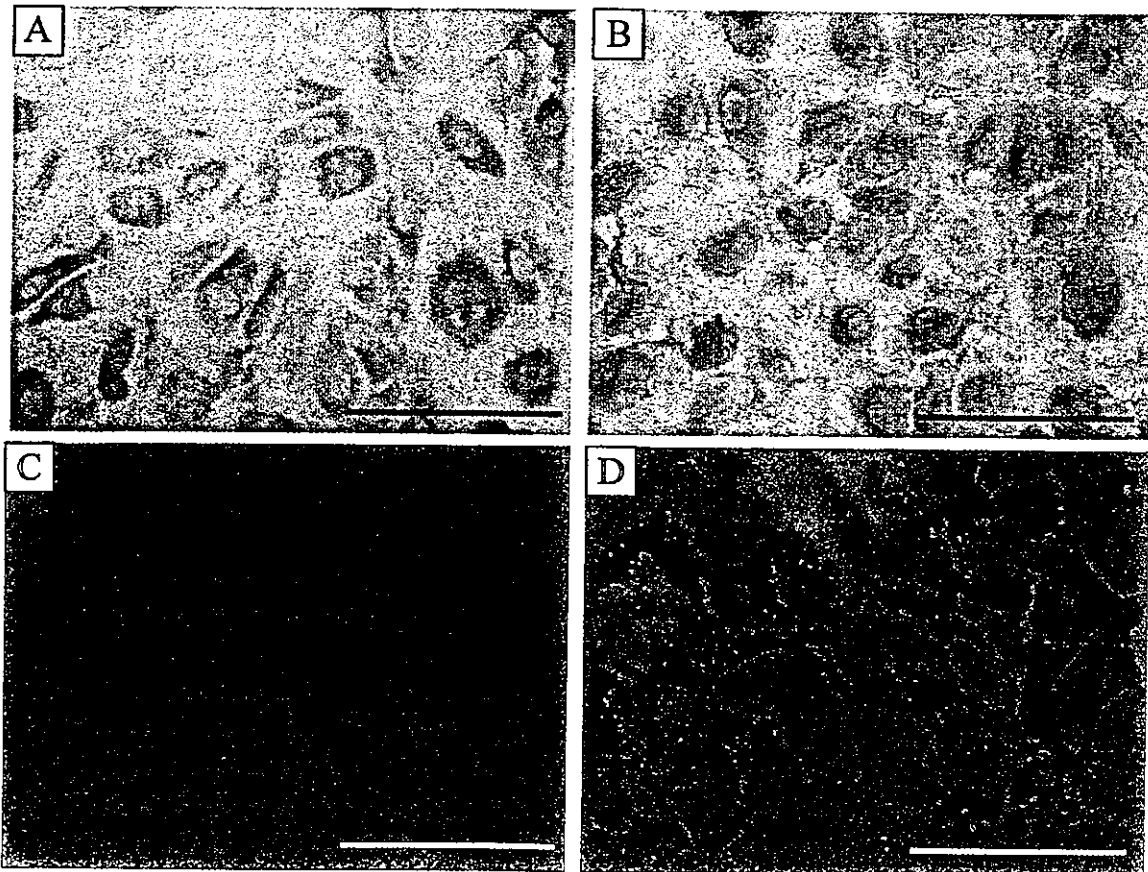


FIG. 4. Histochemical staining of EC-like cells. (A) Light micrograph of EC-like cells staining positively for Flk-1. (B) Light micrograph of EC-like cells staining positively for vWF. (C) CLSM image of EC-like cells taking up Dil-labeled acetylated LDL. (D) CLSM image of EC-like cells staining positively for an NO-specific fluorescence indicator, DAF-2DA (original magnification, $\times 400$; bar, 100 μm).

in Fig. 1. Cells residing in the peripheral region of such colonies migrated and proliferated, whereas in all other regions a compact, cobblestone-like monolayered tissue was formed. In the other pattern, cells grew more slowly. Figure 2 show the growth curve of EC-like cells and the calculated population doubling times of these cells. Among the nine samples that produced EC-like colonies, two different types of growth characteristics were observed. In two samples, the EC-like cells had high proliferative potential (mean PDT, 22 h). Six weeks after PBMC seeding, the number of EC-like cells was approximately 4×10^6 , and these cells were allowed to continue growth after the third passage. In contrast, the other seven samples exhibited low proliferative potential; the PDT of these cells ranged from 59 to 3300 h (mean PDT, 1700 ± 1100 h). All of these poorly proliferating cells ceased their growth during the third passage. To exclude the effect of cell density on cell growth, the growth kinetics of highly proliferative cells were re-quantified at a low seeding density (5×10^2 cells/cm²). These cells seeded at a low density exhibited almost the same PDT (mean PDT, 24 h) as that of cells seeded at a high cell density. Figure 3 shows the morphologic difference between highly proliferative cells and poorly proliferative cells. After the second passage, the highly proliferative cells showed a small shape and polygonal monolayer structure similar to that of mature ECs. On the other hand, poorly proliferative cells were observed as large cells with bizarre shapes.

Immunocytochemical studies showed that regardless of the type of proliferative potential, the cells stained positively for both Flk-1 (a receptor for vascular endothelial growth factor, VEGF) and von Willebrand factor, both

of which are EC-specific markers (Fig. 4A and B).^{17,18} The mean percentages of highly proliferative cells (second passage) expressing Flk-1 and vWF were 98.1 and 97.9%, respectively. In addition, almost all of these cells took up fluorescently labeled acetylated LDL, which is an endothelial cell-specific function (Fig. 4C).¹⁹ Furthermore, these cells also produced NO intracellularly, which was proved by intracellular staining with an NO-specific indicator, DAF-2DA (Fig. 4D).

Antithrombotic potential of EC-like cells

The production of antithrombotic substances by highly proliferative EC-like cells was examined using ELISA techniques and compared with that of HUVECs. For the anti-platelet substance, the amount of eNOS expressed by highly proliferative EC-like cells was approximately one-third of that expressed by HUVECs (EC-like cells, 1100 ± 530 pg/10⁶ cells; HUVECs, 3300 ± 670 pg/10⁶ cells; $p < 0.05$; Fig. 5A). The amount of 6-keto-PGF₁- α was approximately one-half that of HUVECs (EC-like cells, 93 ± 46 pg/10⁶ cells per 24 h; HUVECs, 190 ± 45 pg/10⁶ cells per 24 h; $p < 0.05$; Fig. 5B). As for the fibrinolytic substance, the amount of tPA secreted by EC-like cells was almost identical to that secreted by HUVECs (32 ± 20 and 30 ± 12 ng/10⁶ cells per 24 h; $p = 0.5$; Fig. 5C).

EC-like cell-seeded small-diameter vascular graft

When highly proliferative EC-like cells were seeded onto a small-diameter vascular graft (Fig. 6A) coated with a photocured gelatinous layer as shown in Fig. 6B, a

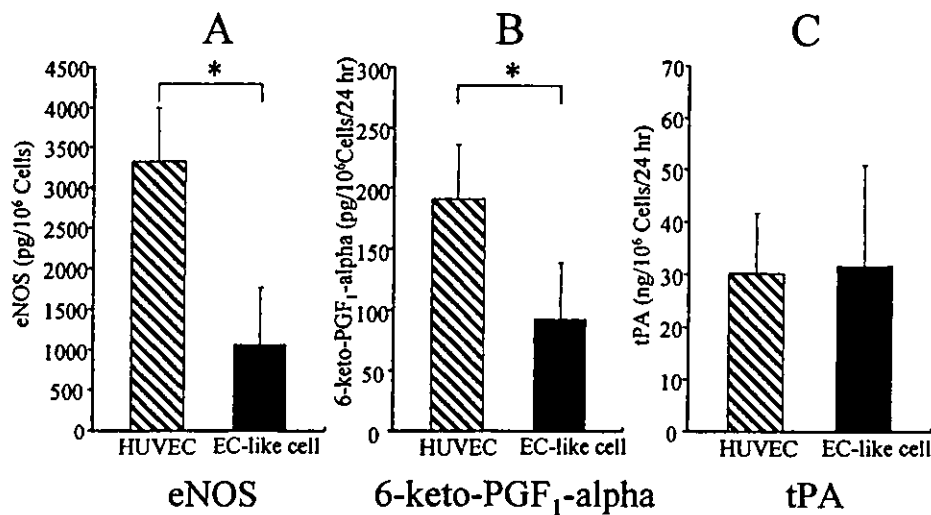


FIG. 5. Antithrombotic potentials of highly proliferative EC-like cells and HUVECs, as measured by ELISA. (A) Expression of eNOS by HUVECs ($n = 4$) and EC-like cells ($n = 4$); * $p < 0.05$. (B) Production of 6-keto-PGF₁- α by HUVECs ($n = 4$) and EC-like cells ($n = 4$); * $p < 0.05$. (C) Production of tPA by HUVECs ($n = 4$) and EC-like cells ($n = 4$); $p = 0.5$. Data represent means \pm SD.

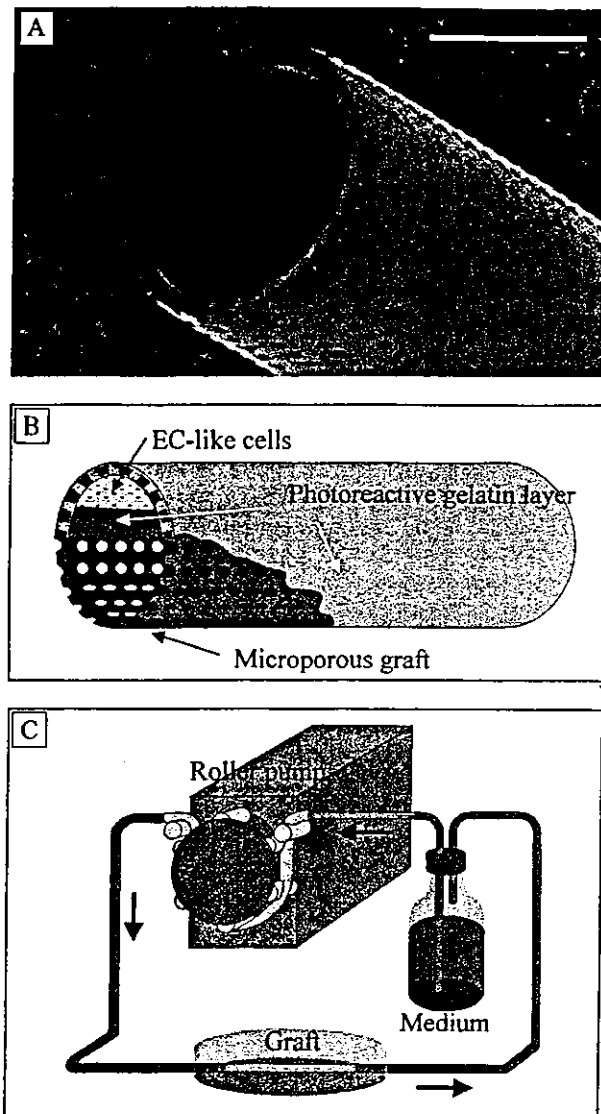


FIG. 6. (A) Scanning electron micrograph of the microporous polyurethane graft. The inner diameter of the graft is 1.5 mm; the wall thickness is 100 μm , and the diameter of each micropore is 100 μm . Bar, 1 mm. (B) Schematic of the prototype model of an EPC-seeded hybrid graft. Photoreactive gelatin is layered and photocured on the surface of the microporous graft and EC-like cells are seeded on the luminal surface of the graft. (C) *Ex vivo* circulatory loop system used to expose the EC-like cell seeded vascular graft to hydrodynamic shear stress. Arrows indicate direction of flow.

cobblestone-like monolayered luminal structure of the graft was obtained after a 4-day culture (Fig. 7A). When hydrodynamic shear stress (30 dyn/cm^2) was applied to the graft for 12 h, using the closed circulatory loop apparatus shown in Fig. 6C, EC-like cells elongated and aligned in the direction of flow. These cells adhered tightly to each other to maintain the high integrity of their confluent monolayer structure and almost all areas were cov-

ered with a cell monolayer (SEM observation; data not shown), similar to that of native artery (Fig. 7B and C).

DISCUSSION

Endothelial cells, which represent the only cell type with antithrombogenic potential among the many living cell types in the body, and which reside at the interface between blood and vascular tissue, are essential for the maintenance of homeostasis of the vascular wall. Therefore, *ex vivo* endothelialization on the luminal surface of artificial grafts exhibits high patency after implantation. This reliable patency has been well proved experimentally and clinically. Deutsch *et al.* have been continuously implanting autologous EC-lined grafts in patients according to well-defined procedures and clinical criteria.³ However, the major limitations of this tissue-engineering approach are in harvesting ECs from the veins of patients and in obtaining sufficient ECs to completely cover the luminal surface of the artificial graft, as well as in surgical intervention before surgical operation for graft implantation.

As a new source of ECs, the harvesting of EPCs from peripheral blood seems to be ideal because it involves minimal invasion. Studies have demonstrated that the hemangioblast is a common progenitor for both hematopoietic cells and endothelial cells.⁴⁻⁶ EPCs share the same cell surface marker, CD34, with hematopoietic stem cells. CD34-positive cells are present in bone marrow,⁵ umbilical cord blood,²⁰ and the peripheral blood mononuclear cell fraction.⁴ Because cells in the PBMC fraction can be separated by the density gradient method, EPCs can be separated from whole blood in the same manner.

Our results showed that there are two types of EC lineage cells in the mononuclear cell fraction of peripheral blood: highly proliferative EC-like cells (population doubling time of 22 h, which is comparable to that of HUVECs of primary culture), which have small and polygonal morphology, and poorly proliferative cells (average population doubling time of 1700 ± 1100 h), which have large and bizarre shapes similar to senescent cells.²¹ Lin *et al.*⁷ indicated that highly proliferative ECs in peripheral blood are derived from bone marrow, whereas the others are of vascular wall origin, as determined by *in situ* hybridization analysis of blood samples from gender-mismatched bone marrow transplant recipients. These results strongly suggest that highly proliferative EC-like cells are EPCs and poorly proliferative cells are "fall-out" ECs.

It appears that purified EPCs may be reasonably obtained from peripheral blood by cell sorting. However, peripheral blood contains only a small number of EPCs. Peichev *et al.*⁶ were unable to detect EPCs in human peripheral blood by flow cytometry analysis and hence it

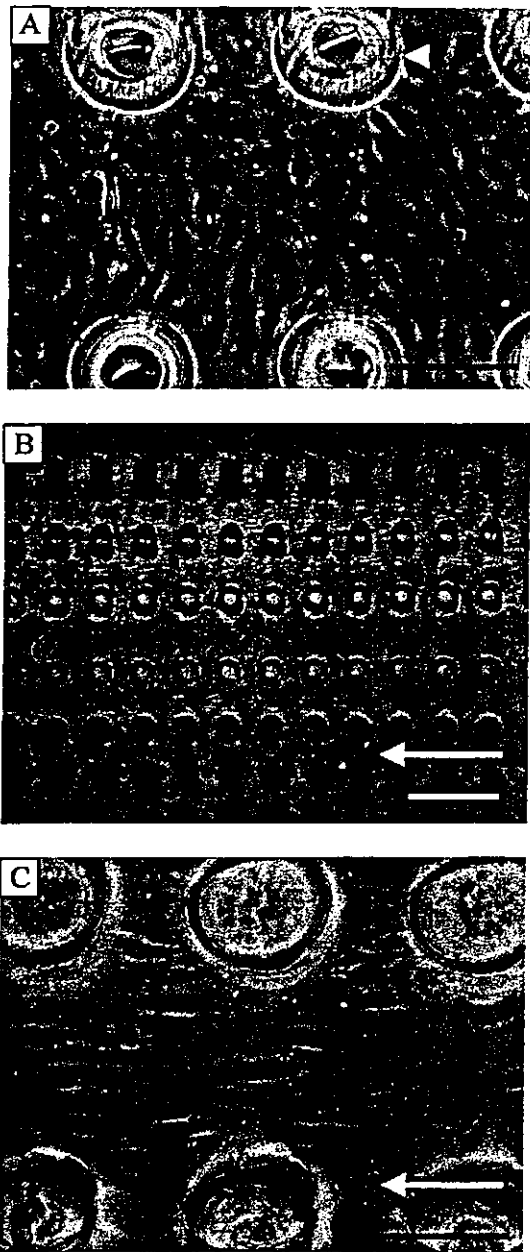


FIG. 7. Phase-contrast micrographs of highly proliferative EC-like cell-seeded vascular graft. (A) Luminal surface of the graft after 4 days of culture under static conditions. EPCs grew to form a cobblestone-like monolayer. Arrowhead indicates micropore of the graft (original magnification, $\times 200$; bar, $100\ \mu\text{m}$). (B) After shear stress loading ($30\ \text{dyn}/\text{cm}^2$, 12 h), EPCs maintained confluent cell-layer coverage on the luminal surface of the microporous vascular graft (flow is indicated by the arrow; original magnification, $\times 100$; bar, $200\ \mu\text{m}$). (C) EPCs were elongated and aligned in the direction of flow (flow is indicated by the arrow; original magnification, $\times 200$; bar, $100\ \mu\text{m}$).

may be difficult to obtain enough purified cells to culture from peripheral blood. Furthermore, cell sorting involves complex procedures that may influence cell viability and their ability to differentiate into ECs. Her-

nandez *et al.*²² showed that CD34-positive cells obtained from PBMCs by using magnetic beads did not develop into EC colonies. In addition, Asahara *et al.*⁴ indicated that coincubation of CD34-positive cells with CD34-negative cells of PBMCs increased the proliferation rate of EPCs to more than 10 times that of CD34-positive cells plated alone. Thus, at this time it may be more effective to culture all cells of the PBMC fraction and exclude senescent ECs in order to obtain *ex vivo*-expandable EPCs from peripheral blood.

In this study, only 18% of highly proliferative cell samples yielded colonies. Hernandez *et al.*²² also showed that EC colonies developed from only 4 of 13 samples of PBMC cultures (40–293 mL). It is possible that the small number of EPCs in PBMCs and their low capability to develop EC colonies (5–12%)²³ are responsible for the difficulty in obtaining highly proliferative cells. Furthermore, EPCs may have no ability to adhere in the early stage of culture.^{6,9,23} Thus, the first exchange of medium may also influence the development of colonies. Further examination is needed to solve these problems before the clinical application of peripheral blood-derived EPCs becomes possible.

Human EPCs thus harvested and cultured had high antithrombogenic potential, similar to that of mature ECs: approximately one-half the antiplatelet function and almost the same degree of fibrinolytic function as mature ECs (Fig. 6). Both NO and PGI₂ are potent inhibitors of platelet activation.^{10,11} In addition, these bioactive substances play a significant role in vasodilation.^{24,25} In general, NO release from ECs is increased on exposure to high shear stress.²⁶ Therefore, EPC-seeded synthetic artificial grafts may exhibit high NO release in response to hydrodynamic shear stress in a shear stress-loaded arterial circulating system. A study by Kaushal *et al.* showed that EPC-seeded decellularized porcine vessels implanted in sheep, and subjected to preconditioning under hydrodynamic shear stress before implantation, exhibited high patency, rapid vascular wall regeneration, contractile activity, and NO-inducing vasodilation similar to those of native artery.⁹ Thus, a vessel was regenerated structurally, morphologically, and functionally. Our implantation study using a canine EPC-seeded compliant graft⁸ exhibited high patency (all grafts [$n = 6$] were patent 3 months postimplantation) and tissue regeneration similar to that of EC-seeded compliant grafts. Taking these results into consideration, it is anticipated that EPCs isolated and expanded *ex vivo* will acquire mature antiplatelet function during *ex vivo* preconditioning by shear stress loading or with the passage of time postimplantation. That is, the nonthrombogenic potential of EPC-seeded grafts may be caused by the complete differentiation of EPCs into ECs with implantation time and/or by synergistic shear stress-induced enhancement of antithrombogenicity. Once EPCs differentiate into ECs and

smooth muscle cells (SMCs) are recruited to the area beneath the endothelium, homogeneous and heterogeneous cell-cell interactions will enhance the integrity of the vascular wall as well as its antithrombotic potential. For example, SMCs will release a peptide, adrenomedullin, that promotes endothelial NO release.²⁷

In general, the mechanical stimulation of ECs will modulate cell shape, the cytoskeleton, and expression of adhesion molecules, all of which function to resist hydrodynamic shear stress.^{13,14} Such stress-induced biomechanical functional and structural adaptation may also be realized in EPC-seeded grafts. In fact, our experiment has shown that under hydrodynamic shear stress EPCs elongate and align themselves in the direction of flow, and that these cells maintain their confluent monolayer structure with high integrity, similar to native artery. In conclusion, EPCs are definitely a potential cell source for tissue-engineered vessels that will be applied clinically in the near future.

ACKNOWLEDGMENTS

This study is financially supported by the Promotion of Fundamental Studies in Health Science of the Organization for Pharmaceutical Safety and Research (OPSR), grant 97-15, and in part by a Grant-in-Aid for Scientific Research (A2-12358017 and B2-12470277) from the Ministry of Education, Culture, Sports, Science, and Technology of Japan. The authors thank Dr. Toshinobu Sajiki for his suggestion of the ELISA method and immunocytochemistry, and Yumiko Miura for her contribution to preparation of laboratory materials and cell culture.

REFERENCES

- Herring, M., Gardner, A., and Glover, J. A single-staged technique for seeding vascular grafts with autogenous endothelium. *Surgery* **84**, 498, 1978.
- Laube, H.R., Duwe, J., Rutsh, W., and Konertz, W. Clinical experience with autologous endothelial cell-seeded polytetrafluoroethylene coronary artery bypass grafts. *J. Thorac. Cardiovasc. Surg.* **120**, 134, 2000.
- Deutsch, M., Meinhart, J., Fischlein, T., Preiss, P., and Zilla, P. Clinical autologous in vitro endothelialization of infrainguinal ePTFE grafts in 100 patients: A 9-year experience. *Surgery* **126**, 847, 1999.
- Asahara, T., Murohara, T., Sullivan, A., Silver, M., van der Zee, R., Li, T., Witzenbichler, B., Schatteman, G., and Isner, J.M. Isolation of putative progenitor endothelial cells for angiogenesis. *Science* **275**, 964, 1997.
- Shi, Q., Rafii, S., Wu, M.H., Wijelath, E.S., Yu, C., Ishida, A., Fujita, Y., Kothari, S., Mohle, R., Sauvage, L.R., Moore, M.A.S., Storb, R.F., and Hammond, W.P. Evidence for circulating bone marrow derived endothelial cells. *Blood* **92**, 362, 1998.
- Peichev, M., Naiyer, A.J., Pereira, D., Zhu, Z., Lane, W.J., Williams, M., Oz, M.C., Hicklin, D.J., Witte, L., Moore, M.A.S., and Raffi, S. Expression of VEGFR-2 and AC-133 by circulating human CD34⁺ cells identifies a population of functional endothelial precursors. *Blood* **95**, 952, 2000.
- Lin, Y., Weisdorf, D.J., Solovey, A., and Hebbel, R.P. Origins of circulating endothelial cells and endothelial outgrowth from blood. *J. Clin. Invest.* **105**, 71, 2000.
- He, H.B., Shirota, T., Yasui, H., and Matsuda, T. Circulating endothelial precursor based compliant hybrid vascular grafts. Abstract presented at the 13th World Congress of the International Society for Artificial Organs, Osaka, Japan, 2001.
- Kaushal, S., Amiel, G.E., Guleserian, K.J., Sharipa, O.M., Perry, T., Sutherland, F.W., Rabkin, E., Moran, A.M., Schoen, F.J., Atala, A., Soker, S., Bischoff, J., and Mayer, J.E. Functional small-diameter neovessels created using endothelial progenitor cells expanded *ex vivo*. *Nat. Med.* **7**, 1035, 2001.
- Radomski, M.W., Palmer, R.M.J., and Moncada, S. The role of nitric oxide and cGMP in platelet adhesion to vascular endothelium. *Biochem. Biophys. Res. Commun.* **148**, 1482, 1987.
- Moncada, S., and Vane, J.R., Arachidonic acid metabolites and the interactions between platelets and blood-vessel walls. *N. Engl. J. Med.* **300**, 1142, 1979.
- Cines, D.B., Pollak, E.S., Buck, C.A., Loscalzo, J., Zimmerman, G.A., McEver, R.P., Pober, J.S., Wick, T.M., Konkle, B.A., Schwartz, B.S., Barnathan, E.S., McCrae, K.R., Hug, B.A., Schmidt, A., and Stern, D.M. Endothelial cells in physiology and in the pathophysiology of vascular disorders. *Blood* **91**, 3527, 1998.
- Urbich, C., Walter, D.H., Zeiher, A.M., and Dimmeler, S. Laminar shear stress upregulates integrin expression. *Circ. Res.* **87**, 683, 2000.
- Girard, P.R., and Nerem, R.M. Shear stress modulates endothelial cell morphology and F-actin organization through the regulation of focal adhesion-associated proteins. *J. Cell. Physiol.* **163**, 179, 1995.
- Kojima, H., Nakatsubo, N., Kikuchi, K., Kawahara, S., Kirino, Y., Nagoshi, H., Hirata, Y., and Nagano, T. Detection and imaging of nitric oxide with novel fluorescent indicators: Diaminofluoresceins. *Anal. Chem.* **70**, 2446, 1998.
- Doi, K., Nakayama, Y., and Mastuda, T. Novel compliant and tissue-permeable microporous polyurethane vascular prosthesis fabricated using an excimer laser ablation technique. *J. Biomed. Mater. Res.* **31**, 27, 1996.
- Yamaguchi, T.P., Dumont, D.J., Conlon, R.A., Breitman, M.L., and Rossant, J. *flk-1*, an *flt*-related receptor tyrosine kinase is an early marker for endothelial cell precursors. *Development* **118**, 489, 1993.
- Rand, J.H., Gordon, R.E., Sussman, I.I., Chu, S.V., and Solomon, V. Electron microscopic localization of factor-VIII-related antigen in adult human blood vessels. *Blood* **60**, 627, 1982.
- Voyta, J.C., Via, D.P., Butterfield, C.E., and Zetter, B.R. Identification and isolation of endothelial cells based on their increased uptake of acetylated-low density lipoprotein. *J. Cell Biol.* **99**, 2034, 1984.

20. Murohara, T., Ikeda, H., Duan, J., Shintani, S., Sasaki, K., Eguchi, H., Onituka, I., Matsui, K., and Imaizumi, T. Transplanted cord blood-derived endothelial precursor cells augment postnatal neovascularization. *J. Clin. Invest.* **105**, 1527, 2000.
21. Borg-Capra, C., Fournet-Bourguignon, M.P., Janiak, P., Villeneuve, N., Bidouard, J.P., Vilaine, J.P., and Vanhoutte, P.M. Morphological heterogeneity with normal expression but altered function of G proteins in porcine cultured regenerated coronary endothelial cells. *Br. J. Pharmacol.* **122**, 999, 1997.
22. Hernandez, D.A., Townsend, L.E., Uzieblo, M.R., Haan, M.E., Callahan, R.E., Bendick, P.J., and Glover, J.L. Human endothelial cell cultures from progenitor cells obtained by leukapheresis. *Am. Surg.* **66**, 355, 2000.
23. Gill, M., Dias, S., Hattori, K., Rivera, M.L., Hicklin, D., Witte, L., Girardi, L., Yurt, R., Himmel, H., and Rafii, S. Vascular trauma induces rapid but transient mobilization of VEGFR2⁺AC133⁺ endothelial precursor cells. *Circ. Res.* **88**, 167, 2001.
24. Palmer, R.M.J., Ferrige, A.G., and Moncada, S. Nitric oxide release accounts for the biological activity of endothelium-derived relaxing factor. *Nature* **327**, 524, 1987.
25. Majerus, P.W. Arachidonate metabolism in vascular disorders. *J. Clin. Invest.* **72**, 1521, 1983.
26. Govers, R., and Rabelink, T.J. Cellular regulation of endothelial nitric oxide synthase. *Am. J. Physiol. Renal Physiol.* **280**, F193, 2001.
27. Shimekake, Y., Nagata, K., Ohta, S., Kambayashi, Y., Teraoka, H., Kitamura, K., Eto, T., Kangawa, K., and Matsuo, H. Adrenomedullin stimulates two signal transduction pathways, cAMP accumulation and Ca²⁺ mobilization, in bovine aortic endothelial cells. *J. Biol. Chem.* **270**, 4412, 1995.

Address reprint requests to:

Takehisa Matsuda, Ph.D.

Department of Biomedical Engineering

Graduate School of Medicine

Kyushu University

Maidashi, Higashi-ku

Fukuoka 812-8582 Japan

E-mail: matsuda@med.kyushu-u.ac.jp

Tissue-Engineered Cartilage Using an Injectable and *in Situ* Gelable Thermoresponsive Gelatin: Fabrication and *in Vitro* Performance

SHINICHI IBUSUKI, M.D.,^{1,2} YASUO FUJII, Ph.D.,¹ YUKIHIRO IWAMOTO, M.D., Ph.D.,²
and TAKEHISA MATSUDA, Ph.D.¹

ABSTRACT

An injectable and *in situ* gelable scaffold can fully fill the space of cartilaginous defects of complex shapes. The authors attempted to develop a novel injection-driven technique for cartilage repair using a thermoresponsive gelatin, poly(*N*-isopropylacrylamide)-grafted gelatin (PNIPAAm-gelatin). A mixed solution of chondrocytes was isolated from a Japanese white rabbit and PNIPAAm-gelatin was spontaneously solidified at 37°C and cultured. The number of cells in the gel with a poly(*N*-isopropylacrylamide) (PNIPAAm) chain of high molecular weight (1.3×10^5 g/mol) and at low concentration (5 w/v%) remained unchanged irrespective of culture time, and minimal cell death and little cell proliferation were observed. A round-shaped morphology was dominantly restored even at 1 week of incubation. The cell population in the G₀/G₁ phase was high (more than 90%), and this gradually increased with culture time. Type II collagen and sulfated glycosaminoglycan (s-GAG) were detected in the tissue-engineered cartilage, but a small amount of type I collagen was also detected. Total collagen and s-GAG increased in level close to those of native hyaline cartilage over 12 weeks of culture. Mechanical properties of the tissue-engineered cartilage responding to loading and unloading of compression force tend to approach those of native hyaline cartilage with culture time. These results suggest that PNIPAAm-gelatin may be a suitable *in situ* formable scaffold for cartilage repair.

INTRODUCTION

ARTICULAR CARTILAGE is a connective tissue responsible for load bearing in synovial joints. Articular cartilage has a limited capacity for self-repair once it has been damaged, regardless of whether or not the damage involves subchondral bone.^{1,2} Although various surgical techniques and strategies for cartilage repair, such as abrasion,^{3,4} osteochondral drilling,^{5,6} and mosaicplasty,⁷ have been attempted, these techniques have had limited success. Transplantation of isolated chondrocytes has re-

ceived increasing interest with respect to cartilage repair,^{8,9} as it appears to provide a promising strategy for filling the defects with *ex vivo* or *in situ* formed cartilaginous tissue. Such cellular or tissue-engineering technology is applied using *in vitro* expanded cells, biocompatible three-dimensional (3-D) matrices, and scaffolds made of natural or artificial extracellular matrices (ECMs). In general, there are two different types of transplantation procedure: the first involves injection of a chondrocyte suspension or a mixed solution of chondrocytes and an injectable scaffold to form an *in situ*

¹Department of Biomedical Engineering, Graduate School of Medicine, Kyushu University, Higashi-ku, Fukuoka, Japan.

²Department of Orthopedic Surgery, Graduate School of Medicine, Kyushu University, Higashi-ku, Fukuoka, Japan.

formable tissue-engineered tissue, and the other involves implantation of an *in vitro* cultured and preconstructed tissue-engineered tissue in which chondrocytes are inoculated and cultured. The former enables manufacture of implants that fit cartilaginous defects with complex shapes, which is of great advantage over the latter. In the former method, injectable substances such as fibrin glue,¹⁰ calcium alginate,¹¹ vinyl group end-capped poly(ethylene oxide),^{12,13} and poly(ethylene oxide)-poly(propylene oxide)-poly(ethylene oxide) triblock copolymer (Pluronic)^{14,15} are used as a scaffold or matrix. These injectable scaffolds are converted from a solution to gel by enzymatic action, chelation, photopolymerization, and thermal gelation, respectively. Pluronic is frequently used as an injectable and *in situ* gelable matrix, which does not exhibit cell adhesiveness in nature.

The authors previously prepared PNIPAAm-gelatin, a thermoresponsive gelatin, that serves as a thermoresponsive artificial extracellular matrix.¹⁶⁻¹⁸ The structural features of PNIPAAm-gelatin are as follows: PNIPAAm as a graft chain is a well-known thermoresponsive polymer,¹⁹ which is grafted on the gelatin molecule. The PNIPAAm polymer is fully hydrated or soluble in aqueous solution below 32°C, but precipitates above this temperature. When its concentration is relatively high, the solution solidifies spontaneously at physiological temperature. On the other hand, gelatin as a main chain of PNIPAAm-gelatin, thermally denatured collagen, is a cell-adhesive protein and is soluble in water at physiological temperature. The combination of this cell-adhesive main chain with thermoresponsive graft chains provides unique function, making it suitable for use as an injectable scaffold. An aqueous solution of PNIPAAm-gelatin is transparent at room temperature, but immediately solidifies at physiological temperatures, as shown in Fig. 1. This injectable property may serve for building a scaffold that fits defects of any shape in living tissues, as well as the induction of homogeneous cell distribution within a 3-D artificial matrix.

The goal of this study is to develop a novel system for cartilage repair, using thermoresponsive gelatin and chondrocytes. The procedure is that a suspension of chondrocytes in PNIPAAm-gelatin solution solidifies *in situ* in the defects of articular cartilage, constructing a tissue-engineered cartilage that completely replicates the defect's space and possibly adheres to the subchondral bone and adjacent cartilage. In this article, the first of a series of our studies, we focus on determining the various potentials of the thermoresponsive gelatin as an injectable scaffold for *in vitro* cartilage repair. We demonstrate the formation of an *in situ* gelable tissue-engineered cartilage, observing morphogenetic aspects both at the cellular level and at the tissue level. The former includes cell proliferation potential, cell morphology, cell cycle, and cell redifferentiation, and the latter includes ECM pro-

duction and mechanical properties. Finally, we discussed the potential of this tissue-engineered cartilage.

MATERIALS AND METHODS

Preparation of poly(N-isopropylacrylamide)-grafted gelatin

PNIPAAm-gelatin was synthesized as previously reported.¹⁶⁻¹⁸ Briefly, dithiocarbamate-derivatized gelatin (DC-gelatin) was first synthesized as follows: 4-(*N,N*-diethylthiocarbamyl)methyl benzoic acid (16.5 g, 58.1 mmol) dissolved in 80 mL of an aqueous sodium hydroxide solution (1.0 N) was neutralized to about pH 8.3; 600 mL of 1-ethyl-3-(3-dimethylaminopropyl)carbodiimide hydrochloride (WSC; Wako, Osaka, Japan), in phosphate-buffered saline (PBS), was added and the mixture was stirred for 1 h at 4°C. Then, 300 mL of gelatin solution (0.1 w/v% gelatin [molecular weight: 9.5×10^4 g/mol; Wako] in PBS) was added and the mixture was stirred for 14 days at room temperature. This mixture was dialyzed with a dialysis membrane (size 36; Wako) and then lyophilized to produce DC-gelatin. The degree of dithiocarbamylation was determined with an ultraviolet/visible (UV/VIS) spectrophotometer (DU 530; Beckman Instruments, Fullerton, CA) at 280 nm. Next, an aqueous solution of *N*-isopropylacrylamide (NIPAAm, 150 mM; Tokyo Chemical Industry, Tokyo, Japan) with DC-gelatin (0.05 mM) was placed in a quartz tube. A stream of dry nitrogen was introduced through a gas inlet to sweep the tube for 10 min. The solution was irradiated by a 400-W Hg lamp (AH400RP; UV Company, Saitama, Japan) in nitrogen atmosphere for 10 or 30 min. PNIPAAm-gelatin was obtained by dialysis and subsequent lyophilization. The molecular weight of the produced PNIPAAm graft chain was estimated as a previously reported.¹⁸

Chondrocyte isolation and expansion

Chondrocytes were isolated from rabbit articular cartilage by the method previously described.²⁰ Articular cartilage slices collected from the knee and hip joints of Japanese white rabbits (11–13 weeks old) were minced. After washing three times in PBS, the slices were digested first in 0.1 w/v% trypsin solution for 30 min, and then in 0.05 w/v% collagenase solution (collagenase N-2; Nitta Gelatin, Osaka, Japan), which was prepared in the following growth medium, for 6–8 h at 37°C in a 50-mL centrifuge tube. The growth medium was Dulbecco's modified Eagle's medium (DMEM; Life Technologies, Rockville, MD) containing 10% fetal bovine serum (FBS; Life Technologies), 10 mM HEPES buffer, 44 mM NaHCO₃, penicillin (50 IU/ml), and streptomycin (50 µg/ml). The cells obtained from the digestion solution

were suspended in the growth medium, filtered through a 70- μm nylon cell strainer (Becton Dickinson Labware, Franklin Lakes, NJ), washed three times with the growth medium, and centrifuged at $300 \times g$ for 5 min at 4°C. The cells were expanded by monolayer culture in a 5% CO₂ atmosphere at 37°C, subcultured two times with trypsin treatment for cell expansion, and fed with fresh growth medium twice a week.

Three-dimensional cell culture in PNIPAAm-gelatin gels

Three-dimensional cell cultures were performed in PNIPAAm-gelatin gel in a 5% CO₂ atmosphere at 37°C with culture medium exchanged twice a week. The culture medium was growth medium supplemented with L-ascorbic acid (50 $\mu\text{g}/\text{mL}$). PNIPAAm-gelatin was dissolved in the culture medium to give a final concentration of 10% PNIPAAm-gelatin in the culture medium. The cells, which were passaged three times in monolayer culture, were collected by centrifugation ($300 \times g$, 4°C, 5 min), washed three times with culture medium, and diluted with culture medium at room temperature to 3.0×10^7 cells/mL ($2 \times$ concentration). This suspension was mixed with an equal volume of 10% PNIPAAm-gelatin solution at 4°C to give a final cell concentration of 1.5×10^7 cells/mL in 5% PNIPAAm-gelatin solution. The mixture was placed in a 12-well cell culture cluster (Corning, Corning, NY) and incubated for 10 min at 37°C for gelation, and then poured together with the culture medium at 37°C on a Microwarm plate (Kitazato, Shizuoka, Japan).

Relative DNA content

The cell numbers in the tissue-engineered cartilages were determined by measuring the amount of DNA in enzyme-digested samples. Three-dimensional cultures were performed in various kinds of PNIPAAm-gelatin hydrogels as shown in Table 1. The DNA of the samples were extracted with a QIAamp DNA minikit (Qiagen, Hilden, Germany). Aliquots of the digest were mixed, using a PicoGreen dsDNA quantitation kit (Molecular

Probes, Eugene, OR). Fluorescence emission was measured with a Molecular Imager FX (Bio-Rad Laboratories, Hercules, CA). Phage γ DNA, as supplied in the kit, was used as a standard.

In situ fluorescence viability study

To assess chondrocyte viability in the tissue-engineered cartilages, an *in situ* fluorescence viability study was performed with a Live-Dead viability/cytotoxicity kit (Molecular Probes). The tissue-engineered cartilages in the two-well Lab-Tek chamber slide (Nalge Nunc, Naperville, IL) were first washed three times with PBS at 37°C on the Microwarm plate, and 200 μL of the combined 2 μM calcein AM and 4 μM ethidium homodimer 1 reagents (Molecular Probes) were added. The mixture was then incubated at 37°C for 40 min, and 200 μL of PBS was added. Next, the cells stained with the combined Live/Dead assay reagents were observed by confocal laser scanning microscopy (CLSM) (Radiance 2000; Bio-Rad Laboratories).

Cell morphology

The appearance of cells in the tissue-engineered cartilages was observed by CLSM and scanning electron microscopy (SEM) (JSM 840A; JEOL USA, Peabody, MA). The samples were first washed three times with PBS at 37°C on the Microwarm plate, and 200 μL of 2 μM calcein AM solution (Molecular Probes) was added; the mixture was then incubated at 37°C for 40 min, and 200 μL of PBS was added. Next, the cells stained with calcein AM were observed by CLSM. The cultured tissues were fixed with 1% glutaraldehyde–1.44% paraformaldehyde in buffer at 37°C for 60 min, frozen in liquid nitrogen, and lyophilized. Specimens for SEM were sputter coated with an alloy of platinum and palladium, and observed by SEM.

Cell cycle

The percentages of cells in G₀/G₁ phase relative to all cells in the 3-D and monolayer cultures were measured

TABLE I. CODE NAMES OF FOUR KINDS OF PNIPAAm-GELATIN GELS PREPARED AT DIFFERENT CONCENTRATIONS OF PNIPAAm-GELATIN WITH DIFFERENT MOLECULAR WEIGHTS OF PNIPAAm GRAFT CHAINS

Code name	Concentration of PNIPAAm-gelatin solution (w/v%)	Molecular weight of PNIPAAm-graft chains
Gel A	5	1.3×10^5
Gel B	10	1.3×10^5
Gel C	5	5.0×10^4
Gel D	10	5.0×10^4

by flow cytometry (FACSCalibur; Becton Dickinson, San Jose, CA).²¹ Propidium iodide (PI) (CycleTest Plus DNA reagent kit; Becton Dickinson)-stained cells were prepared according to the manufacturer's instructions and analyzed by flow cytometry. The samples were washed three times with PBS, minced, and digested first in 0.1% trypsin solution for 30 min and then in 0.05 w/v% collagenase solution (collagenase in DMEM with 10% FBS) for 1–2 h at 37°C in a centrifuge tube. Moreover, subconfluent cells in monolayer culture were also collected by trypsin treatment. After collecting the cells by centrifugation (300 × *g* for 5 min at 4°C), the nuclei of the cells were isolated and stained with PI, as supplied in the CycleTest Plus DNA reagent kit (Becton Dickinson), according to the kit manual. Nuclear DNA content was measured on the basis of PI fluorescence, using a 488-nm argon laser and FACSCalibur flow cytometry. Fluorescence was acquired in the linear mode (10,000 events) and the results were analyzed with CellQuest and Mod-Fit LT (Becton Dickinson). The percentages of G₁ (2N), S (2–4 N), and G₂ + M (4N) chondrocytes were calculated on the basis of defined gates for each population.

Macroscopic analysis, histology, and immunohistochemistry

For macroscopic analysis of the tissue-engineered cartilage, the tissue was observed at room temperature without any fixation. For histological evaluation, the tissue-engineered cartilages were rinsed in PBS at 37°C, fixed with 1% glutaraldehyde–1.44% paraformaldehyde in buffer at 37°C for 2 h, dehydrated in a graded series of alcohols at 37°C, embedded in paraffin, and sectioned at 5- μ m thickness. Deparaffinized serial sections were stained with Safranin-O/Fast Green (Wako) to detect accumulated s-GAG. For immunohistochemistry,²² the sections were deparaffinized, treated with 0.1% trypsin at 37°C for 30 min, and washed three times with PBS. The sections were then treated with testicular hyaluronidase (1.45 IU/mL, type I-S; Sigma, St. Louis, MO) and chondroitinase ABC (0.25 IU/mL; Sigma) at 37°C for 30 min prior to incubation with primary antibodies. All primary antibodies were diluted with PBS containing 0.1% Triton X-100 (Sigma) and 0.7% carrageenan (Sigma). As primary antibodies, the mouse monoclonal antibody against rabbit type I collagen [Anti-hCL (I); Daiichi Fine Chemicals, Toyama, Japan] and the mouse monoclonal antibody against rabbit type II collagen [Anti-hCL (II); Daiichi Fine Chemicals] were applied to the sections. The antiserum to type I collagen was used at 1:100 dilution (5 μ g/mL protein concentration) and that to type II collagen at 1:1000 dilution (500 ng/mL protein concentration). The incubation time was overnight at room temperature. After washing with PBS, the sections were applied with a biotinylated rabbit anti-mouse IgG anti-

body (Nichirei, Tokyo, Japan), and incubated at room temperature for 60 min. After washing with PBS, the sections were immersed in 150 mL of methanol with 1.5 mL of H₂O₂, and incubated at room temperature for 60 min. After washing again with PBS, the sections were applied with streptavidin-conjugated immunoperoxidase (Nichirei). The signal was finally visualized as a brown reaction product from the peroxidase substrate 3,3'-diaminobenzidine (DAB; Merck, Darmstadt, Germany).

Biochemical analysis

The amounts of s-GAG in the tissue-engineered cartilages were quantitated with a Simple s-GAG quantitation kit (Hokudo, Sapporo, Japan). The tissue-engineered cartilage and rabbit articular cartilage were homogenized and digested with an enzyme solution, as supplied in the kit, at 60°C for 3 hr. After the extraction, 100 μ L of each sample was mixed with 1.3 mL of the dye reagent and shaken with a Vortex mixer. The absorbance of the samples were measured at a wavelength of 630 nm, using the UV/VIS spectrophotometer. Chondroitin sulfate C (Sigma) for plotting the calibration curve was used in this experiment. Data were normalized by the wet weight (wet wt.) of the tissues.

Total collagen content of the enzyme-digested samples was also quantitated with a Sircol collagen assay kit (Accurate Chemical & Scientific, Westbury, NY).²³ The tissue-engineered cartilage and rabbit articular cartilage were homogenized in 0.5 N acetic acid and digested with pepsin (1 mg/mL) in 0.5 N acetic acid for 24 h at 4°C before inactivation of the pepsin by the addition of tris(hydroxymethyl)aminomethane (Tris) to a final concentration of 50 mM and titration to neutral pH with concentrated NaOH. The pepsin-resistant residue was extracted for an additional 24 h in 0.15 M NaCl containing 20 mM dithiothreitol (DTT) and 50 mM Tris-HCl at pH 7.4 in the presence of a protease inhibitor cocktail (P 8340; Sigma). The pepsin digest and DTT extracts were combined and concentrated in an Ultrafree-15 concentrator (Millipore, Bedford, MA) with a molecular cutoff of 30,000. This sample was prepared for assay by mixing with Sircol dye reagent for 30 min on an orbital shaker. The samples were then centrifuged to collect the collagen–dye complex. The dye bound to the collagen pellet was solubilized with an alkali reagent, and the absorbance of the samples was measured at a wavelength of 540 nm, using the UV/VIS spectrophotometer. An acid-soluble type I collagen was used to obtain the calibration curve for this experiment. Data were normalized by the wet weight of the tissues.

Determination of mechanical properties

The mechanical properties of the tissue-engineered cartilage, cultured for up to 12 weeks, were determined

itated at physiological temperature (37°C) to produce an opaque gel at a relatively low concentration (5 w/v%). Figure 1 shows photographs of a cell-incorporated PNIPAAm-gelatin aqueous solution at room temperature and at physiological temperature. The solution immediately (within 10 s) solidified at 37°C. Such a gel had induced little shrinkage within the culture period. The sol-gel phase transition could reversibly occur at an early phase of culture in a cell-incorporated gel (defined as a tissue-engineered cartilage) (Fig. 1a and b). After a prolonged culture period (e.g., a 12-week culture; Fig. 1c) however, the tissue-engineered cartilage remained in gel form even

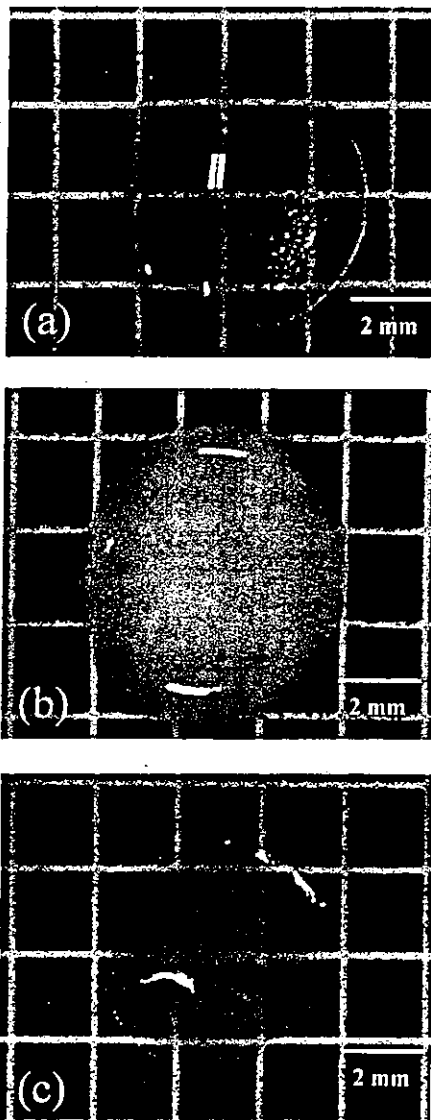


FIG. 1. Macroscopic study of tissue-engineered cartilages. (a) Cell-incorporated PNIPAAm-gelatin solution at room temperature. (b) Cell-incorporated PNIPAAm-gelatin gel is immediately formed at 37°C. (c) Twelve-week-cultured tissue-engineered cartilage at room temperature.

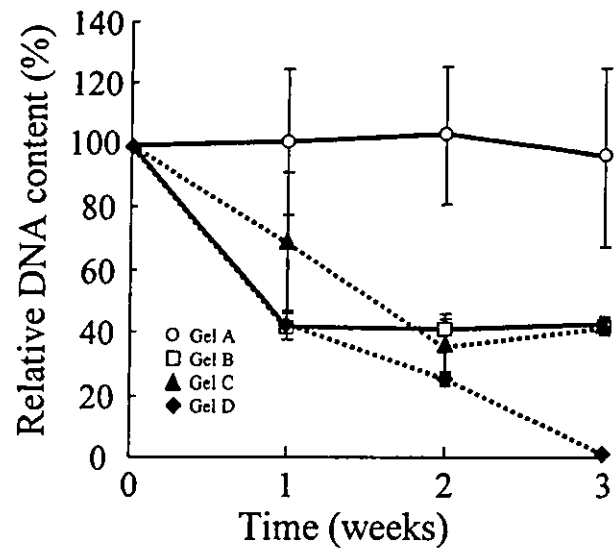


FIG. 2. Relative DNA contents of cells in four kinds of PNIPAAm-gelatin gel ($n = 5$, mean \pm SD): (O, Gel A) Concentration of PNIPAAm-gelatin solution, 5 w/v%; molecular weight of a PNIPAAm graft chain, 1.3×10^5 g/mol; (\square , Gel B) 10 w/v% and 1.3×10^5 ; (\blacktriangle , Gel C) 5 w/v% and 5.0×10^4 ; (\blacklozenge , Gel D) 10 w/v% and 5.0×10^4 .

at room temperature, indicating that it lost thermosensitivity (discussed below).

DNA content and chondrogenic differentiation

It is of paramount importance whether incorporated cells are alive or not in PNIPAAm-gelatin gel. Experiments to determine this were conducted under various conditions at a fixed cell density (1.2×10^7 /mL), but at different concentrations (5 and 10 w/v%) of PNIPAAm-gelatin and different molecular weights (5.0×10^4 and 1.3×10^5 g/mol) of the PNIPAAm graft chain on gelatin. Table 1 lists the four sets of PNIPAAm-gelatin solutions and their code names. Figure 2 shows the time course of changes in relative DNA content of the cells in four different tissue-engineered cartilages. Here, relative DNA content was defined as (DNA content at each stage)/(initial DNA content) \times 100. The highest relative DNA content ($96.6 \pm 29.1\%$) was maintained in gel A (lower concentration and higher molecular weight of the graft chain) for the entire 3 weeks of culture: there was almost no change in DNA content in 3 weeks of culture. However, the DNA content in gel D (higher concentration and lower molecular weight of the graft chain) progressively decreased with culture time, and only low-level DNA content was observed after 3 weeks of culture. An intermediate behavior between the above-mentioned extreme cases was observed in gel B and gel C: after an initial loss (approximately 60%) of DNA content in 1 to 2 weeks of culture, the DNA content did not change after 3 weeks

of culture. Thus, DNA content, and cell numbers in tissue-engineered cartilage, strongly depended on the concentration of PNIPAAm-gelatin and the molecular weight of the graft chain. On the basis of this result, further experiments were performed with gel A.

To visualize the cell viability in gel A as a function of culture period, living and dead cells in PNIPAAm-gelatin gels were fluorescently stained, using viability and cytotoxicity fluorescence probes, respectively. Figure 3 shows confocal laser scanning micrographs of the stained cells cultured for 1 to 3 weeks. At each culture time, living cells (stained green) were predominant, and only a few cells were dead (stained red). Although the living cells had various cell shapes including round-shaped, elongated, and spindle cells at 1 week of culture (Fig. 3a), round-shaped cells became predominant at 3 weeks of culture (Fig. 3b). An example of a round-shaped cell surrounded by a porous scaffold was observed by SEM, which was obtained by freeze-drying and subsequent fracture of the tissue-engineered cartilage (Fig. 4).

Cell cycles of the cells harvested from monolayer culture under subconfluent conditions (approximately 60%) and PNIPAAm-gelatin gels were analyzed by flow cytometry. The data of flow cytometry show the percentages of cell cyclically differentiated cells relative to all of the cells in PNIPAAm-gelatin gels. The percentages of cells arrested in G_0/G_1 phase relative to all of the cells in subconfluent monolayer-cultured cells were $81.0 \pm 0.18\%$, whereas those in the PNIPAAm-gelatin gels at 1 week of culture were $91.7 \pm 0.97\%$ ($p < 0.001$), $93.3 \pm$

0.29% at 2 weeks of culture ($p < 0.001$), and $95.9 \pm 1.1\%$ at 3 weeks of culture ($p < 0.001$) (Fig. 5). These results strongly indicate that most of the cells in PNIPAAm-gelatin gels redifferentiated.

Morphogenesis of tissue-engineered cartilage

Tissue-engineered cartilage cultured for 12 weeks exhibited a semitransparent appearance that resembles that of hyaline cartilage (Fig. 1c). When allowed to stand at room temperature, such tissue-engineered cartilages did not dissolve, indicating that extracellular matrices (ECMs) secreted by cells appear to restore the integrity of tissue-engineered cartilages.

Safranin O/Fast Green-stained tissue sections had a distribution of metachromatic matrices, s-GAG, a product of differentiated chondrocytes, throughout the tissue (Fig. 6a). In these sections, most of the cells were homogeneously distributed and exhibited a round-shaped morphology. In addition, characteristic lacunae of differentiated chondrocytes were also observed around each cell. Immunostained tissue sections demonstrated that type II collagen was positively stained throughout the tissues (Fig. 6b). On the other hand, little deposition of type I collagen was observed (Fig. 6c).

The biochemical composition of the tissue-engineered cartilage was analyzed as a function of culture period (1, 2, 4, 8, and 12 weeks). The amount of total collagen in the tissue-engineered cartilage continuously increased with culture time, reaching 4.5 ± 1.0 ($\mu\text{g}/\text{mg}$ wet wt. of the tissue) at 12 weeks (Fig. 7a). The amount of s-GAG

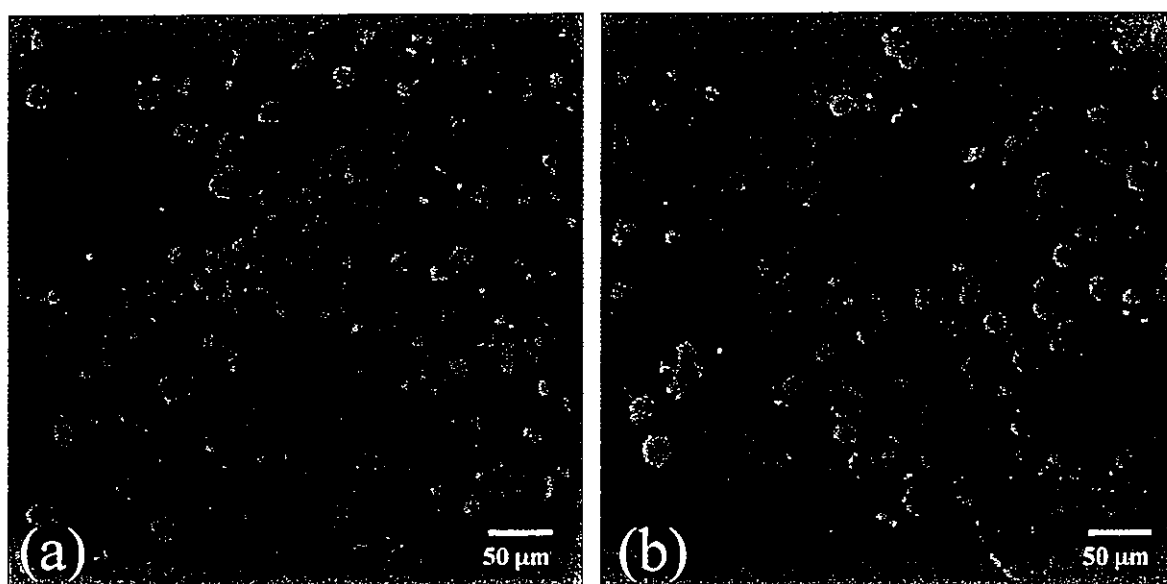


FIG. 3. Fluorescence images used for determining viability and morphology of chondrocytes in PNIPAAm-gelatin gel at (a) 1 week of culture, and (b) 3 weeks of culture: Living cells (stained green) and dead cells (stained red) were stained with calcein AM and ethidium homodimer 1, respectively.

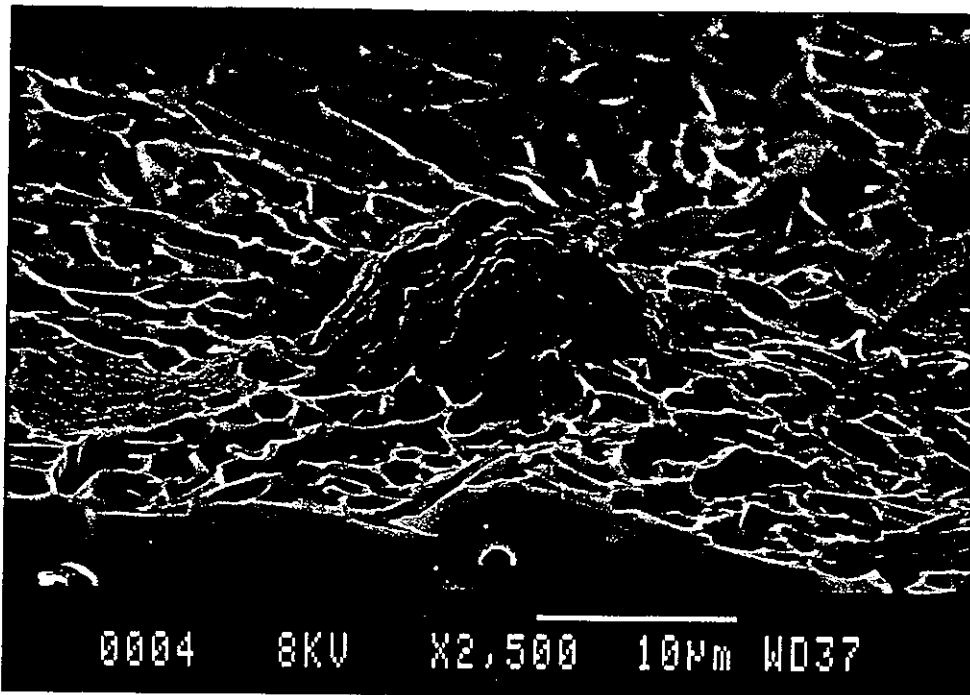


FIG. 4. Morphology of cell entrapped in PNIPAAm-gelatin gel, observed by SEM (24 h of culture).

remained at a low level in the initial 2 weeks; however, after that, it continuously increased up to 13.9 ± 1.0 ($\mu\text{g}/\text{mg}$ wet wt. of the tissue) at 12 weeks (Fig. 7b). The amounts of total collagen and s-GAG of normal articular cartilage were 23.1 ± 5.1 and 15.8 ± 0.1 ($\mu\text{g}/\text{mg}$ wet wt. of the tissue), respectively.

Mechanical properties of tissue-engineered cartilage

The measurement of mechanical properties of the tissue-engineered cartilages provides information about how closely the tissue-engineered cartilages resemble na-

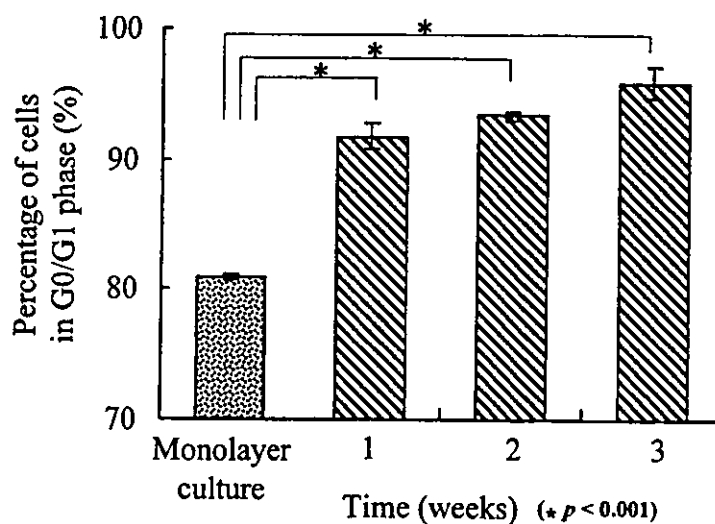


FIG. 5. Percentages of cells in G₀/G₁ phase relative to all the cells in the tissue-engineered cartilage were significantly ($p < 0.001$) higher than that of monolayer-cultured cells under subconfluent conditions, and tended to increase with culture time ($n = 3$, mean \pm SD). Statistical analysis was performed by ANOVA.

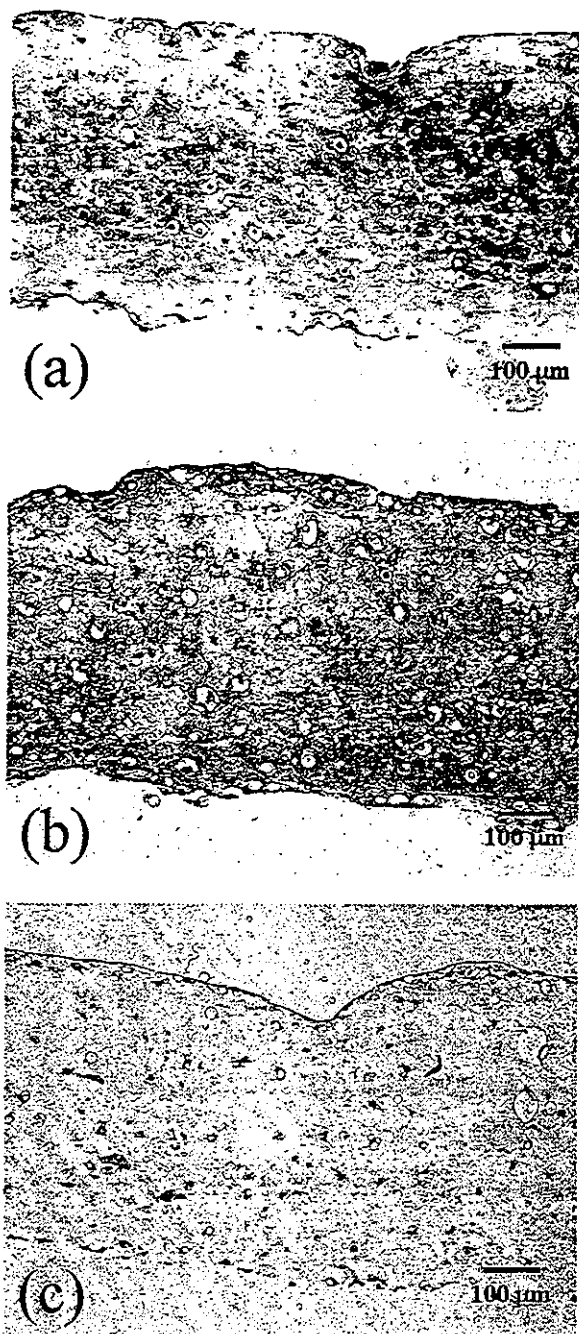


FIG. 6. Histological analysis of tissue-engineered cartilage cultured for 12 weeks. Samples were stained with (a) Safranin O/Fast Green (original magnification, $\times 100$), (b) an antibody against type II collagen (original magnification, $\times 100$), and (c) an antibody against type I collagen (original magnification, $\times 100$).

tive cartilage in terms of mechanical responses on loading and unloading of compression force. That is, the maximum strain on loading and the residual strain on unloading have an inverse relationship to stiffness and recoverability, respectively. The compression force of 2.5

kPa was chosen since early period-cultured tissue-engineered cartilages had mechanically been very weak. Figure 8b shows the time course of changes in strain of the tissue-engineered cartilages that were loaded at 2.5 kPa for the initial 120 s and then unloaded for 480 s. All of the samples were gradually strained for the initial 120 s (stress-loading period), and tended to recover with time (recovery period) after unloading of stress. Each set of data showed the average strain of the samples at each

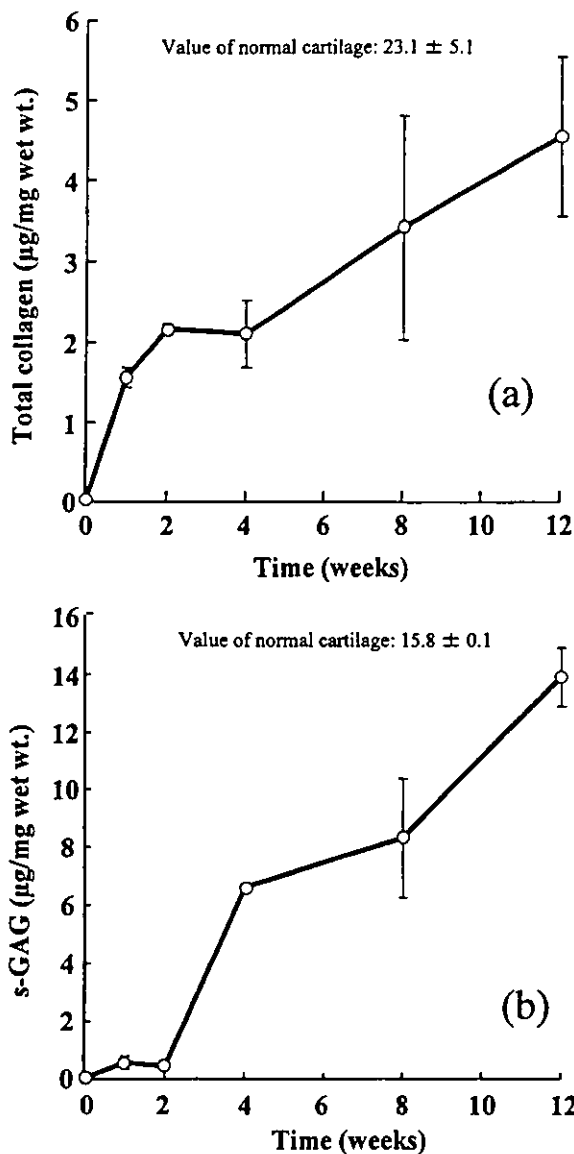


FIG. 7. Time course of changes in the amounts of extracellular matrices in tissue-engineered cartilages ($n = 3$, mean \pm SD). (a) The amount of total collagen measured, using a Sircol collagen assay kit and normalized by wet weight of the tissue. (b) The amount of s-GAG measured, using a Simple s-GAG quantitation assay kit and normalized by wet weight of the tissue.

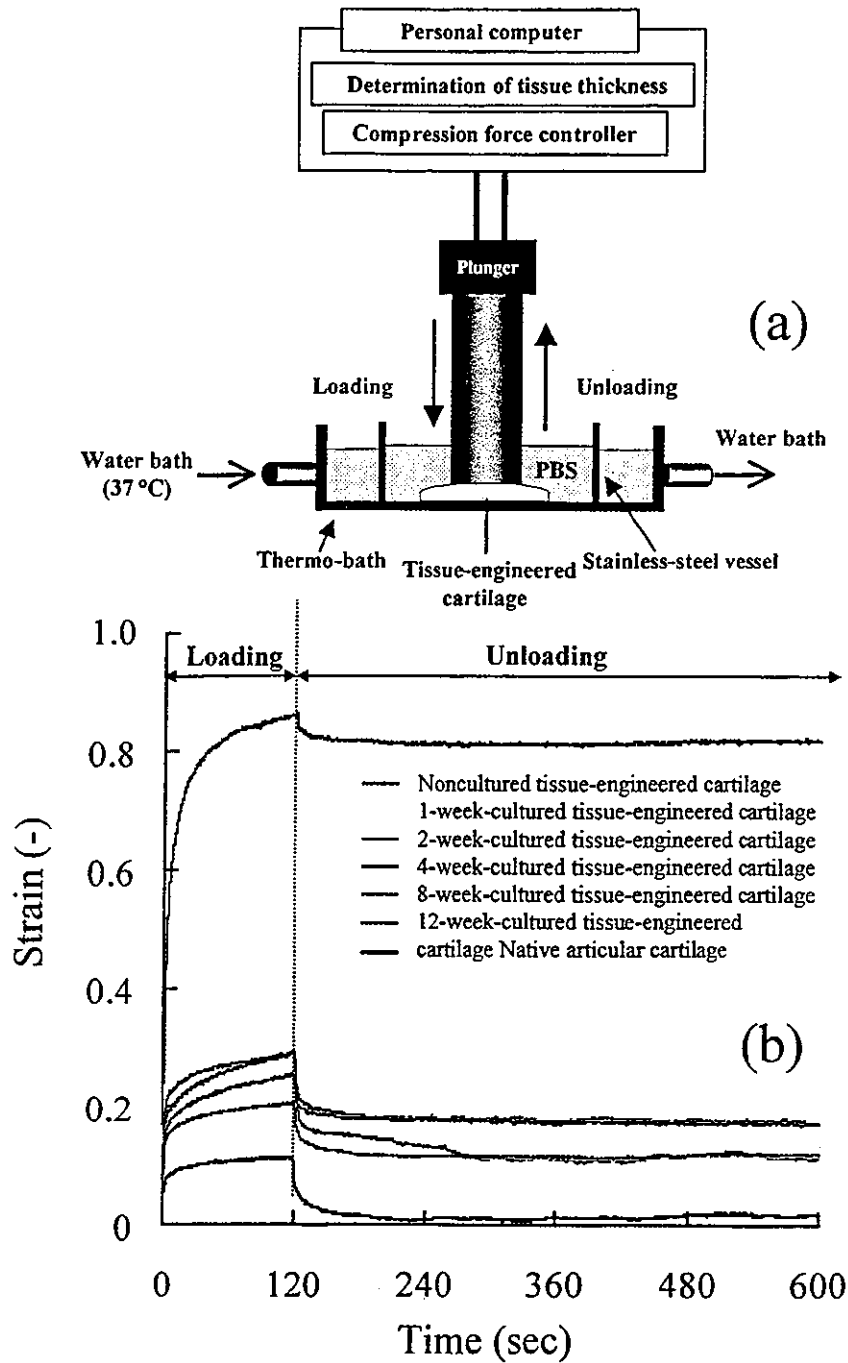


FIG. 8. (a) Schematic of the mechanical loading system, composed of a personal computer for controlled mechanical loading and unloading of tissue-engineered cartilage placed in PBS at 37°C. (b) Time course of changes in the strain of the tissue-engineered cartilages on loading and unloading. The thicknesses of the tissue-engineered cartilages were measured during loading (initial 120 s) and unloading (subsequent 480 s). Each line indicates the average strain of the tissue-engineered cartilages at each culture time ($n = 3$, mean).

stage. The average strain of normal cartilages reached 0.11 ± 0.02 at its peak and recovered to almost zero in a short time (approximately 90 s) after unloading. On the other hand, the average strain of cell-free PNIPAAm-gelatin gel reached 0.86 ± 0.07 at its peak, and showed

little recovery after unloading. For the tissue-engineered cartilages, with an increase in culture period, both the maximum strains during loading and the residual strains during unloading were decreased. The maximum and residual strains of the tissue-engineered cartilages at each

culture period are shown in Fig. 9a and b. Maximum strain of the tissue-engineered cartilages tended to gradually decrease with culture time and become close to that of normal cartilage at 12 weeks. The residual strain also tended to become smaller, and approached that of normal cartilage for the initial 8 weeks; no further decrease in the residual strain was observed beyond this period.

DISCUSSION

Since articular cartilage has a limited capacity for self-repair, a tissue-engineering approach using chondrocytes

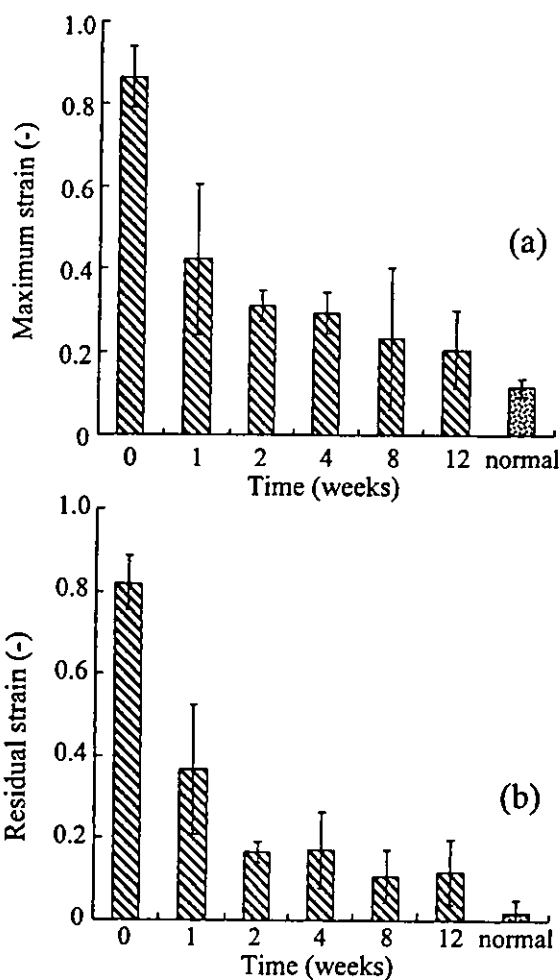


FIG. 9. Mechanical properties of the tissue-engineered cartilages and rabbit articular cartilages in terms of maximum strain and residual strain ($n = 3$, mean \pm SD). (a) Maximum strain indicates the strain of the tissue-engineered cartilages at 120 s. The maximum strains of the tissue-engineered cartilages and normal articular cartilages have an inverse relationship to tissue stiffness. (b) Residual strain indicates the strain of the tissue-engineered cartilages at 600 s. The residual strains of the tissue-engineered cartilages and normal articular cartilages have an inverse relationship to tissue recoverability.

with a preconstructed or injectable scaffold is one promising solution. To this end, numerous studies have been reported.²⁵⁻²⁹ If such an injectable substance can induce *in situ* gelation, a cell-suspended, moldable scaffold can fill the defect's space to form a tissue-engineered cartilage in close contact with adjacent living tissues. An "ideal" injectable scaffold for cartilage repair should meet the following requirements: (1) the injectable substance should be water soluble when a cell-containing injectable solution is poured into defects in tissues, thus enabling the solution to fill defects of complex shapes; (2) such a solution should solidify at a rapid rate under mild conditions that induce little or minimal damage to transplanted cells and adjacent living tissues; (3) a non-shrinkable property after gelation is needed, thereby preventing the generation of an interspace between adjacent living tissues and the tissue-engineered cartilage formed; (4) an appropriate biodegradability is required to replace the obtained scaffold with ECMs produced by cells injected into the tissue-engineered cartilage; (5) nontoxicity of materials and its metabolically degraded substances as well as that of biomaterials in use for the clinical implantations is also required; and (6) the gel-formed scaffold should have suitable mechanical properties withstanding biomechanical stress in a target tissue, since a large mechanical strength against loaded compression force is needed for articular cartilage. In addition to the aforementioned requirements, the following three key issues are also demanded at cellular and tissue levels: (7) high cell viability in the scaffold, (8) cell redifferentiation in a 3-D environment (the dedifferentiated chondrocytes in monolayer culture exhibit fibroblast-like morphology and a high proliferation potential, whereas differentiated cells in normal cartilage should be round-shaped and exhibit low proliferation potential), and (9) phenotypic expressions of specific markers of normal chondrocytes such as type II collagen and s-GAG. As discussed below, PNIPAAm-gelatin appears to fulfill the majority of the requirements mentioned above.

Scheme 2 demonstrates the mechanism of gelation of PNIPAAm-gelatin. First, a fully hydrated, random-coiled PNIPAAm graft chain at room temperature is dehydrated above 34°C, resulting in the spontaneous collapse of the graft chain, which is converted to a compact globule. Spontaneously, intramolecular hydrophobic associations that induce collapse of the entire PNIPAAm-gelatin molecule occur between the compact globules of graft chains. When the concentration of PNIPAAm-gelatin is quite low, the solution becomes not a gel but an opaque solution. At a relatively high concentration, intermolecular aggregations between collapsed PNIPAAm-gelatin globules induce the gelation. In this study, our interest was in whether chondrocytes can survive in a 3-D environment, redifferentiate to normal cells, and produce specific ECMs of hyaline cartilage, and whether the me-